Thermal conductivity of model zeolites: molecular dynamics simulation study

Thermal conductivity of model zeolites: molecular dynamics simulation study

Vladimir V Murashov

Department of Chemistry, University of British Columbia, Vancouver, British Columbia, Canada V6T 1Z1

Abstract. The thermal conductivity of model zeolites was investigated using non-equilibrium molecular dynamics calculations. This type of calculation was found to overestimate the thermal conductivity of low-density silica polymorphs. A better reproduction of the experimental results was found for zeolites, and this was related to the lower phonon mean free path. The thermal conductivity of framework silicates was shown to be determined primarily by the vibrations of the continuous oxygen sublattice. Thus, the most drastic suppression of the heat transfer was related to alterations of the O–O distances; for example, a sixfold reduction in thermal conductivity compared to that of siliceous LTA zeolite was found for LTA-AlPO$_4$. Framework cations were shown to affect the heat transfer by changing the vibrational modes of the structural building units of the framework and non-framework counter-cations, by disturbing the oxygen sublattice locally and acting as Rayleigh and resonant scatterers. A model assuming the heat transfer to be due only to non-dispersive acoustic phonons failed to reproduce the dependence of the thermal conductivity on the mass of the cations and the unit-cell dimension, thus suggesting a more sophisticated mechanism of heat transfer to be operative in framework materials. The effect of non-framework non-ionic species on the thermal conductivity was shown to be determined by their effect on the characteristics of the oxygen framework vibrations. Thus, repulsive interactions between the oxygen sublattice and Xe$_8$ clusters, reducing the anisotropy and anharmonicity of the oxygen vibrations, give rise to enhanced heat transfer in LTA-SiO$_2$ at ambient conditions.

1. Introduction

Thermal conductivity is an important property of matter, characterizing the effectiveness of heat transfer, and knowledge of it is essential in a wide area of scientific forecasting, ranging from the design of new products and materials, and modelling of technological processes, to environmental (e.g. weather prediction) and geophysical calculations (e.g. forecasting of earthquakes). Measurements of thermal conductivity remain non-trivial, especially for particulate solids. Only few experimental studies of a very important class of materials synthesized largely in microcrystalline forms, i.e. zeolites, have been reported (for a review, see reference [1]). There is also controversy as regards whether information about bulk thermal conductivity can be obtained from measurements on particulate materials [2]. Thus, there have been only few studies concerning the effects of structure and composition on the thermal conductivity of framework silicates [3].

In this work, the factors affecting the thermal conductivity of model zeolites with LTA topology (the mnemonic three-letter structure-type codes developed under the authority of the IUPAC [4] are used) are explored using the non-equilibrium molecular dynamics (NEMD) simulation technique, which has been employed successfully in calculations for an arbitrary

1261

one-dimensional anharmonic solid [5], soft-sphere solids [6], and clathrate hydrates [7]. The LTA-topology zeolites were chosen for this study because the temperature dependence of the thermal conductivity at sub-ambient temperatures has become available recently for one of the zeolites with this topology, namely for sodium zeolite A (hereafter denoted as NaA) [1].

2. Details of the simulation procedure

The rigid-ion pairwise isotropic interatomic potentials of Kramer, Farragher, van Beest, and van Santen (abbreviated as KFBS) were employed to model the silica phases and silicates [8,9]. Variable-shape simulation cells containing 192 TO_2 molecular units were used. Nosé constant-pressure [10] and constant-temperature [11] algorithms were employed. The initial positions of the atoms were assigned according to the available experimental structural data for quartz (the unit-cell chemical composition is Si_3O_6) [12], sodium zeolite A [13, 14] (in the modelling of zeolites of the LTA family, the unit-cell chemical composition of NaA is $Na_{96}Al_{96}Si_{96}O_{384}$ and that of LTA-SiO_2 is $Si_{24}O_{48}$), and siliceous faujasite (FAU topology; the unit-cell chemical composition is $Si_{192}O_{384}$) [15]. Xenon atoms were arranged initially to reside at the 8g sites of the LTA topological cell ($Pm\bar{3}m$, $x = 0.337$) forming a cube with the length of the side ≈ 4 Å, giving rise to the unit-cell chemical composition $Xe_8Si_{24}O_{48}$. A fourth-order Gear algorithm with a time step of 0.5 fs was employed to integrate the equations of motion. The Ewald method was used to treat the long-range electrostatic interactions. For each configuration the systems were allowed to equilibrate to achieve a steady state for 10 ps, after which averages were accumulated over subsequent 20 ps trajectories. The thermal conductivity coefficient was calculated using a homogeneous translationally invariant technique [16–18] with an 'external-field strength' of 0.003 Å^{-1} (test runs showed that the system response is linear at this strength of the external perturbation). The enthalpic term in the definition of the energy flux was approximated by the sum of the average energies and the virials of the species present in the system [19, 20]. Convergence of the energy flux function was achieved within 40 ps to 80 ps.

3. Results and discussion

Calculations of the thermal conductivity tensor of the quartz polymorph of silica at 300 K and 0.1 MPa showed that NEMD employing the KFBS potential tends to overestimate the experimental values; that is, the calculated thermal conductivity coefficient parallel to the *c*-axis of the quartz structure is 16 W m^{-1} K^{-1} compared to the experimental value of 10.4 W m^{-1} K^{-1} [21], and the values for the thermal conductivity coefficient parallel to the *a*-axis are 8.2 W m^{-1} K^{-1} and 6.21 W m^{-1} K^{-1} (calculated and experimental, respectively). At the same time, calculations predict a lower density for quartz (see table 1). This overestimation of the thermal conductivity of quartz in these calculations can be related to the presence of structural defects in the experimental samples of quartz. The deficiencies of the calculation technique (this issue requires further investigation) and the potential model, which was shown to overestimate the frequencies of the bending modes of silica tetrahedra [22], and the destabilization of the low-density polymorphs and the stabilization of the high-density polymorphs [23] can also affect the accuracy of the calculations.

On the other hand, the thermal conductivity of dehydrated sodium zeolite A was reproduced in the calculations using experimentally determined unit-cell parameters to within the uncertainty of the data, i.e. the calculated value is 0.6 W m^{-1} K^{-1} compared with the bulk thermal conductivity of 0.65 W m^{-1} K^{-1} estimated from experimental measurements for particulate material [26]. This closeness of the calculated and experimental values can be

Table 1. Comparison of the calculated and experimental structures and energies (relative to those of quartz or quartz-like phases) for silica phases and zeolites at 300 K and 0.1 GPa. The experimental thermodynamic data are from reference [24], and the references for the experimental structural data are given in the table.

Parameter		Quartz	FAU-SiO$_2$	LTA-SiO$_2$	LTA-AlPO$_4$
a/Å					
	Calculated	4.94(7)	24.68(12)	12.05(3)	24.40(7)
	Experimental	4.913(5)	24.2576(3)		23.782(6)
c/Å					
	Calculated	5.44(4)			
	Experimental	5.405(5)			
ρ/g cm^{-3}					
	Calculated	2.60	1.275	1.367	1.338
	Experimental	2.647	1.3420		1.445
Symmetry		$P3_12$	$Fd\bar{3}m$	$Pm\bar{3}m$	$Fm\bar{3}c$
Reference		[12]	[15]		[25]
$\Delta E(\Delta H)$/kJ mol^{-1}					
	Calculated	0	70	62	92
	Experimental	0	13.6		15.55

partially explained by the shortening of the phonon mean free path in silicates due to additional phonon scattering on point defects [27]. At the lowest temperatures investigated, when the phonons travel furthest between collisions, the phonon mean free path in silicates can be between those observed in quartz and amorphous silica—that is, between $\approx$100 Å and 3 Å at 100 K [28]—leading to the reduction of the effect of the artificial limit on the distance that phonons can travel between collisions set by the size of the MD box.

To investigate the effects of the structure and chemical composition of silicates and related phases on the thermal conductivity, purely siliceous zeolites (zeosils) were considered initially. The effect of the openness of the structure on the thermal conductivity was investigated with siliceous faujasite (hereafter referred to as FAU-SiO$_2$), as its synthesis has been reported and it is characterized by a relatively simple cubic lattice [15]. Siliceous faujasite has one of the lowest densities among the known silica polymorphs, and has very small Si–O–Si angles (138.4°) in its structure [29]. The presence of these small angles was correlated with the destabilization of the silica framework [30]. Therefore, the effect of the framework structure on the thermal conductivity can be expected to be pronounced. The reported lattice unit-cell parameter of the siliceous faujasite at room temperature correlates fairly well with the value obtained in the $N\sigma T$-calculations (see table 1). Remarkably, MD simulation also correctly predicts a negative coefficient of thermal expansion, in agreement with earlier calculations employing different potentials [31]: the calculated lattice cell parameter increased by 0.02 Å with the decrease of the temperature from 300 K to 100 K, while experimental studies show an increase by 0.0247 Å on cooling to 5 K [15]. The calculated normalized volume change is given in figure 1.

On the other hand, the excess lattice energy of siliceous faujasite (compared with the lattice energy of quartz) is significantly overestimated, which is normal for the potential model employed [23]. The calculated temperature dependence of the thermal conductivity is given in figure 2. The lattice thermal conductivity has a negative temperature coefficient,
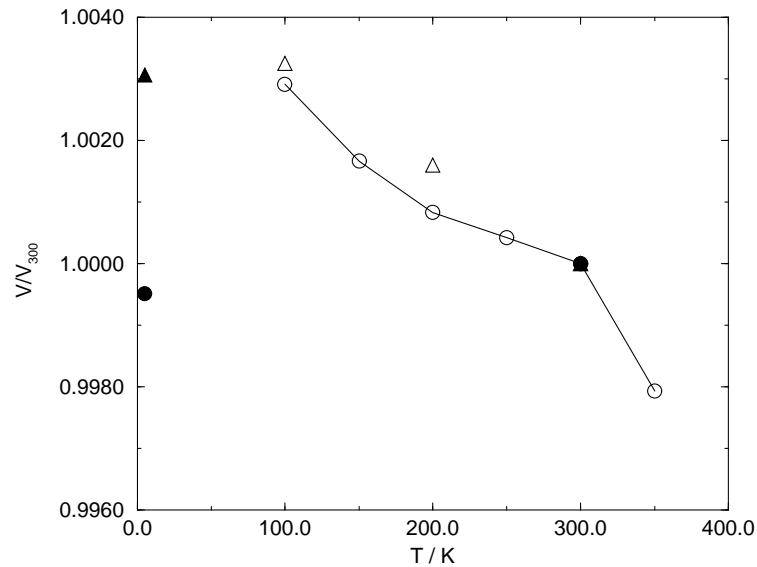
Figure 1. The temperature dependence of the normalized unit-cell volume of FAU-SiO$_2$ (triangles) and LTA-SiO$_2$ (circles). Filled symbols denote experimental points (from [15] for FAU-SiO$_2$ and [14] for NaA) and open symbols represent calculated values. V_{300} is the unit-cell volume at ambient conditions.
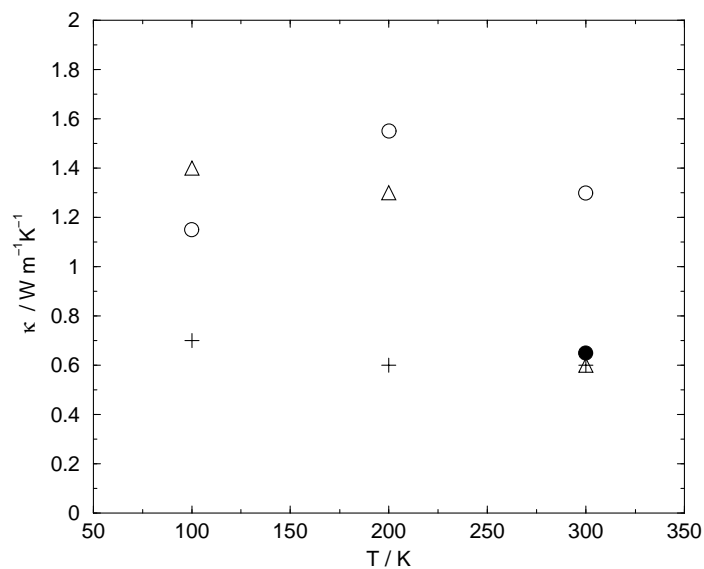

Figure 2. The calculated temperature dependence of the bulk thermal conductivity of zeolites. Circles represent LTA-SiO$_2$ (the $N\sigma T$-ensemble), crosses represent NaA (the NVT-ensemble), and triangles represent FAU-SiO$_2$ (the $N\sigma T$-ensemble). The filled circle denotes the experimental data point for NaA taken from reference [26].

characteristic of a simple crystalline solid over the temperature range between 100 and 300 K. At lower temperatures, calculated values can deviate significantly from experimental values. These classical MD simulation studies fail to reproduce the thermal properties of systems for

which quantum effects become substantial. As a result of these effects, the low-temperature dependence of the thermal conductivity of the crystalline solids determined mainly by the heat capacity dependence has a positive temperature gradient.

The LTA-topology zeolite has not been synthesized in a purely siliceous form, but it was considered in this study in view of the availability of experimental measurements of the thermal conductivity for its substituted form (namely NaA) [1]. This framework material was chosen to elucidate the effects of framework and non-framework substitution. The calculated doubled unit-cell parameter of LTA-SiO_2 (see table 1) is smaller than the experimental unit cell of zeolite NaA at the ambient conditions (a(NaA) $= 24.555(5)$ Å) [13], as can be expected for substitution for silicon atoms with aluminium which has a larger ionic radius. The calculated negative volume thermal expansion of this phase contradicts the small increase in the unit-cell parameter with temperature change from 5 K to 300 K observed experimentally for NaA [14]. In addition, an anomaly is observed in the calculated temperature dependence of the unit-cell volume in the temperature range between 200 K and 350 K (see figure 1), which is similar to that found for a second-order displacive temperature-induced phase transformation, e.g. those of cristobalite and quartz [32]. On the other hand, conservation of the cubic dimensional symmetry during the temperature-induced phase transformation of LTA-SiO_2 indicates that this transformation may be similar to the experimentally observed pressure-induced displacive-type phase transformation in NaA [33]. In the lower-temperature phase, the $[SiO_4]^{4-}$ tetrahedra are trigonally deformed (elongated along one of the threefold axes). As a result, a symmetrical distribution of the relatively rigid O–Si–O angles observed at 350 K becomes split into two distributions centred at around 105° and 110° in the low-temperature phase, and a sharp peak of the first coordination sphere of the O–O radial distribution function observed at high temperatures shows a shoulder corresponding to larger separations [1]. In contrast, FAU-SiO_2 exhibits differentiation of the relatively flexible Si–O–Si angles at low temperatures, and does not show noticeable deformation of the tetrahedral units upon simulated cooling.

Deformation of oxygen tetrahedra and differentiation of the O–O distances in the low-temperature phase of LTA-SiO_2 can account for the calculated reduction of the thermal conductivity coefficient at $T < 200$ K (see figure 2). Notably, the calculated temperature dependence of the thermal conductivity of LTA-SiO_2 (i.e. the temperature at which the thermal conductivity reaches its maximum) agrees well with the experimental data for NaA [1]. Evolution of a framework structure similar to the temperature-induced one could be responsible for the negative density dependence of the thermal conductivity of this phase observed in the calculations at 300 K (see figure 3). This negative pressure coefficient of thermal conductivity is not unique, and has been observed in experimental measurements on another material with a tetrahedral framework, ice [34], which also exhibits negative thermal expansion.

The calculated thermal conductivity of LTA-SiO_2 is around 1.3 W m^{-1} K^{-1} at ambient conditions, which is higher than that of FAU-SiO_2 (0.6 W m^{-1} K^{-1}), in good correlation with the lower density of the latter. Earlier studies indicated almost linear density dependence of the thermal conductivity for silica and related phases [35].

The temperature dependence of the thermal conductivity of the LTA and FAU-type zeolites is determined by two competing processes: increase of the phonon mean free path with decreasing temperature, and increasing anisotropy of the motions of oxygen atoms leading to irregularities of the oxygen sublattice (such as trigonal deformation of the oxygen tetrahedra in LTA zeolites) and to the reduction of the density (see above). Dominance of the former yields T^{-1}-dependence of the thermal conductivity, while the latter effect results in a more positive power of the temperature term in the thermal conductivity dependence. The lessening of the temperature dependence in these framework materials becomes pronounced at $T < 200$ K (see figure 2).
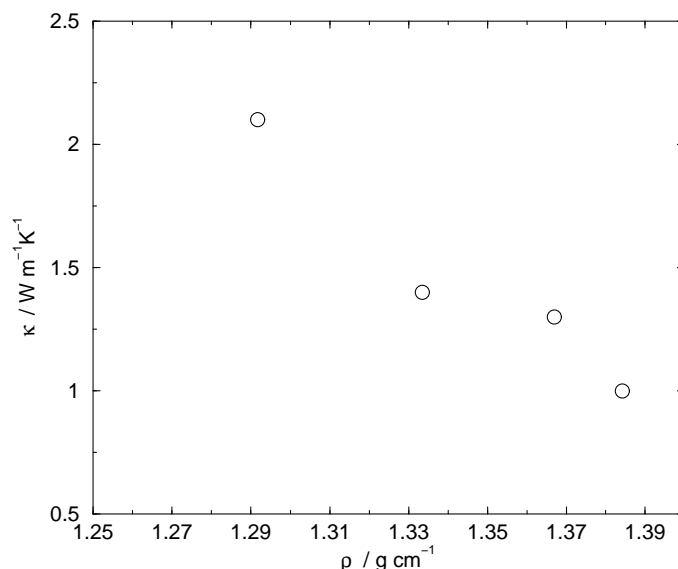
Figure 3. The calculated density dependence of the thermal conductivity of LTA-SiO$_2$ at 300 K.

Distortions of the crystal lattice around imperfections of any kind are known to cause phonon scatter, giving rise to reduction of the heat transport. In this work, only ordered alterations of the lattice were considered. The effect of the isoelectronic substitution of framework cations (e.g. Si for Ge) was investigated by replacement of silicon atoms with model cations characterized by the short-range parameters of aluminium or gallium and by silicon long-range parameters, i.e. silicon ionic charge, and silicon mass. Full substitution (denoted as LTA-A and LTA-G for the aluminium and gallium parameters, respectively) and orderly substitution for only half of the silicon atoms (LTA-SA and LTA-SG) according to Loewenstein's rule [36] were investigated. In accord with the effective ionic radii of aluminium and gallium atoms being larger than that of silicon, the calculated phases of LTA-A, LTA-G, LTA-SA, and LTA-SG have unit-cell parameters (24.19(4) Å, 24.64(8) Å, 24.14(5) Å, and 24.39(8) Å, respectively) larger than that of LTA-SiO$_2$. The O–O radial distribution functions calculated for LTA-SiO$_2$, LTA-SA, and LTA-SG indicate that while the first maximum remains centred at around 2.65 Å, it expands toward larger distances on going from Si to SG (see figure 4). The calculated thermal conductivity coefficient of LTA-A is higher than that of LTA-SiO$_2$ ($\kappa = 1.5$ W m^{-1} K^{-1}) which can be a manifestation of the effect of lower density (see above). Cancellation of this effect and the effect of the more complex structure of LTA-SA compared to LTA-SiO$_2$ yields a thermal conductivity of the former virtually the same as that calculated for the latter. The heat transfer in LTA-SG is the lowest among those of these phases, and can be related to the alterations of the O–O distances within oxygen tetrahedra in addition to the increase of the unit-cell dimensions. This reduction of thermal conductivity is partially offset by a simpler crystal structure of LTA-G, and the heat transfer in this phase appears to be more effective than that in LTA-SG, but less effective than that in LTA-SiO$_2$, i.e. $\kappa = 1.1$ W m^{-1} K^{-1}.

The isoelectronic analogue of silica, aluminium phosphate AlPO$_4$, which has been reported to form a phase with the LTA-type structure (LTA-AlPO$_4$) [37], was calculated to investigate the effectiveness of the heat transfer in these materials. The $N\sigma T$-calculations yielded a phase with cubic symmetry in accord with experimental studies and with the unit-cell
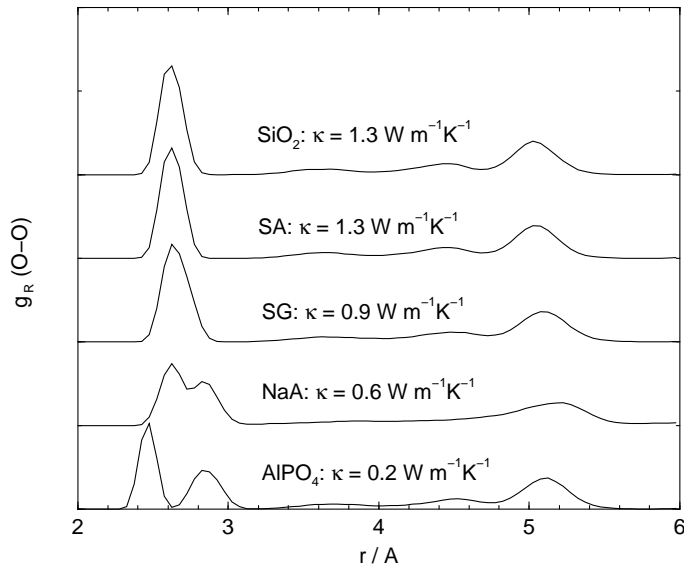
Figure 4. The calculated radial distribution functions for the O–O pair, and values of the coefficient of thermal conductivity of model LTA-topology zeolites at 300 K and 0.1 MPa (for NaA the NVT-calculations employed experimentally determined unit-cell parameters).

parameters exceeding the experimental values [25] by $\approx$3% (see table 1), which agrees with the overestimation observed for the calculations on quartz-like $AlPO_4$ employing the same interatomic potentials [8]. Large differences in the lengths of the Al–O and P–O bonds (that is, $r(Al–O) = 1.74$ Å and $r(P–O) = 1.52$ Å [38]) results in alteration of the oxygen sublattice and a significant reduction of the calculated thermal conductivity coefficient—it can be as low as 0.2 W m^{-1} K^{-1} at 300 K and 0.1 MPa. Indeed, the calculated radial distribution function of the O–O pairs of atoms (see figure 4) shows that in LTA-$AlPO_4$ the peak corresponding to the first coordination sphere is split into two peaks representing smaller $[PO_4]^{3-}$ and larger $[AlO_4]^{5-}$ tetrahedra.

The effect of the differences in masses of the framework cations on the thermal conductivity was also investigated. Similarly to in the investigation of geometric factors, the masses of half of the silicon atoms of the alternating tetrahedral units were changed. This type of substitution did not result in a change of the unit-cell volume. A significant reduction of the thermal conductivity is observed with increase of the differences in masses (see figure 5). This reduction of the high-temperature thermal conductivity with the increase of the mass of the framework cation to $M($'Si'$) = 100$ g mol^{-1} correlates well with the decrease by a factor of 2.5 predicted from the dependence $\kappa \propto M_{ave} V_{atom} \Theta_D^3 n_s^{-2/3} \gamma^{-2}$, where M_{ave} is the mean atomic mass, V_{atom} is the atomic volume, Θ_D is the Debye temperature, n_s is the number of atoms per unit cell, and γ is the Grüneisen parameter, for a relatively rigid framework [39], assuming that the Debye temperature does not change when the cation mass is changed. On the other hand, this formula anticipates a more drastic reduction of the thermal conductivity, namely by a factor of 5 (compared with the reduction observed in the simulation, by a factor of 2.6) for a phase with light 'Si' atoms, i.e. $M($'Si'$) = 1$ g mol^{-1}. It also does not explain the further reduction of the thermal conductivity of LTA-'Si'O_2, for which all silicon atoms were assigned the mass of 100 g mol^{-1}, to 0.3 W m^{-1} K^{-1}, and the increase of the thermal conductivity of the phase with all silicon atoms having the mass 1 g mol^{-1} to 1.6 W m^{-1} K^{-1}. These discrepancies could be
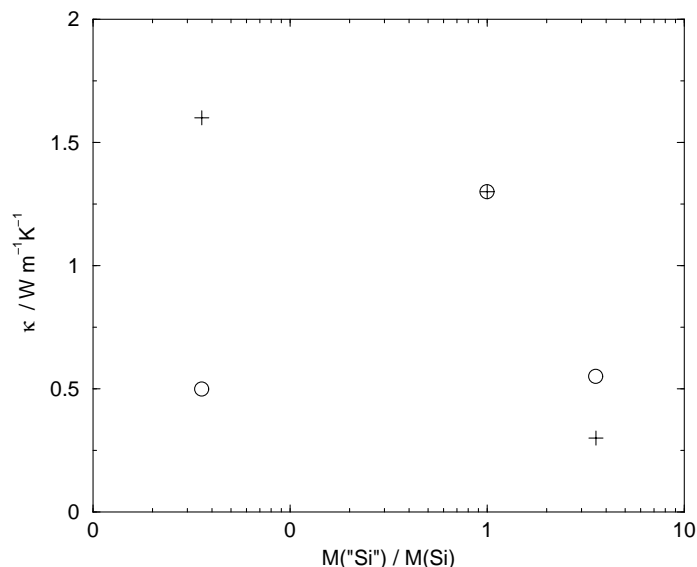
Figure 5. The dependence of the thermal conductivity on the mass ratio of the framework cations. Circles denote half-substituted phases and crosses denote fully substituted phases.

an indication that optical modes in materials with low-density frameworks like silicates cannot be ignored (the assumption that they can be ignored was made in the derivation of the above formula) in the heat transport processes, and that localized vibrations of framework cations (especially heavy ones) can affect the heat transport via resonance scattering of phonons. Such a mechanism of phonon scattering was observed earlier in inclusion compounds [44] and in filled-framework semiconductors with $CoAs_3$ structure [40–42]. Similar results have been observed for a range of dielectric compounds and pure elements [45]. The negative mass coefficient of thermal conductivity could also be an indication that the heat transport in these materials is determined by vibrations of the structural building units, i.e. oxygen tetrahedra enclosing framework cations, and that the increasing mass of such units reduces the vibrational amplitudes of these units, and consequently the anharmonicity and related phonon–phonon coupling.

Heteroelectronic substitution, requiring introduction into the structure of counter-cations to maintain charge balance, was studied for zeolite NaA with a unitary Si/Al ratio (LTA-topology zeolite with the chemical formula describing the unit-cell composition $Na_{96}Al_{96}Si_{96}O_{384}$). In agreement with the experimentally observed distortion of the local structure by counter-cations [46] and the reported structural strains in dehydrated zeolite NaA at ambient conditions [47], the unit cell simulated under constant-stress conditions was severely distorted, although the main features of the LTA topology were preserved. Another feasible explanation of the instability of NaA in the constant-stress calculations lies in the underestimation of the covalency of the Si–O bonding in the pairwise interatomic potentials employed. This is why the thermal conductivity calculations for this phase were performed using a unit-cell parameter fixed at the experimental value, i.e. $a = 24.555(5)$ Å [13]. The calculated value of the thermal conductivity, intermediate between those found for $LTA-SiO_2$ and $LTA-AlPO_4$ (see above), correlates well with the splitting of the first coordination sphere of the O–O pair observed in NaA (see figure 4), which is not as drastic as the splitting observed in $LTA-AlPO_4$. The less-effective heat transfer in the substituted form of the LTA silica phase

could also be related to enhanced phonon scattering on disturbances of the oxygen sublattice caused by framework and non-framework cations. These distortions can act as Rayleigh-type point scatterers of phonons [48]. Calculations also suggest an almost linear temperature dependence of the thermal conductivity of NaA, with a negative slope over the temperature range from 100 K to 300 K (see figure 2).
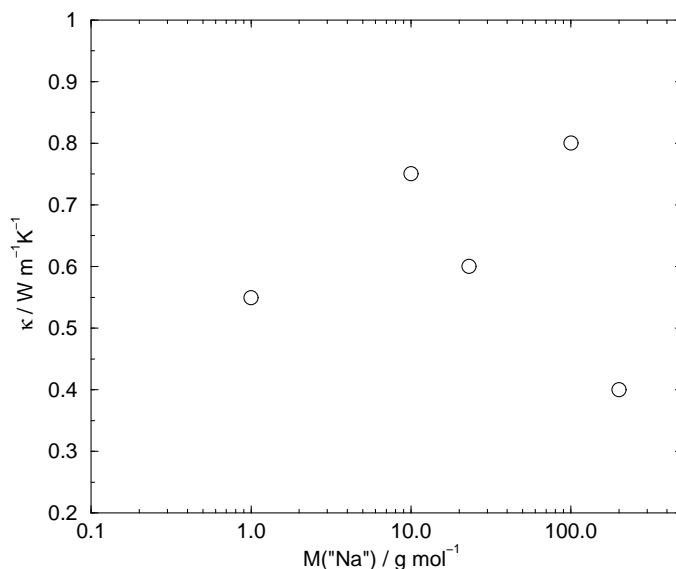

Figure 6. The dependence of the thermal conductivity on the mass of the non-framework cations.

To investigate the possibility of effective phonon scattering on 'rattling' vibrations of heavy non-framework cations similar to those observed in skutterudites [41, 42, 49], sodium cations were substituted for with hypothetical counter-cations with the potential parameters of the sodium cation, but with different masses. The thermal conductivity was found to exhibit a complex behaviour (see figure 6) which can be related to counter-cation vibrations on and off resonance, with framework modes contributing most to the heat transfer. For constant interatomic interactions, the effective vibrational constant of the counter-cations remains unaltered; therefore, their vibrational frequency can be expected to change proportionally to $M(\text{`Na'})^{-1/2}$. Drastic reduction of the thermal conductivity in the presence of heavy counter-cations (>100 g mol^{-1} in this case) could be an indication of the scattering of framework phonons on 'rattling' vibrations of non-framework cations. Vibrations of framework and non-framework cations differ in that the former are confined within structural building units, e.g. oxygen tetrahedra as in low-density silica and silicates, while the latter occupy cavities of the framework structure and have the ability to undergo thermal vibrational motion with very large amplitudes, even hopping between different sites of similar energy separated by low potential energy barriers. This reduction of the thermal conductivity with the mass of the non-framework cations agrees well with correlations found from experimental studies of the thermal conductivity of silicates at ambient conditions [3, 50].

This reduction of the thermal conductivity of the framework materials filled with heavy non-framework species interacting strongly with the framework atoms can be observed for example in zeolites incorporating heavy non-framework cations or encapsulated metal clusters. In particular, this phenomenon has to be considered in studies of the evolution of zeolites used as traps and storage for radioactive isotopes, and in the design of novel materials for electronics.

The possibility of phonon scattering on non-ionic guest clusters similar to that in clathrate hydrates [51] was investigated by considering LTA-SiO$_2$ zeolite with a maximum load of Xe atoms, i.e. eight atoms per α-cage [52]. Incorporation of guest species did not change the unit-cell dimensions, but an increase of the thermal conductivity to 1.65 W m^{-1} K^{-1} at 300 K and 0.1 MPa was exhibited. The repulsive interactions of the xenon atoms with the oxygens can restrict the highly anharmonic and anisotropic vibrational modes that describe the motions of oxygen atoms directed inward in the cavities of the framework structure, and thus might result in the reduction of the phonon–phonon scattering.

4. Conclusions

To summarize, the thermal conductivity of low-density-framework silicates and silicas is determined by vibrations of the propagating oxygen sublattice forming propagating nets of structural polyhedra, and can be affected by alterations of the geometry of this sublattice and the presence of framework and non-framework cations. The former can change the characteristics of the vibrations of the structural building units as a whole, while the latter distort the oxygen sublattice locally and act mainly as Rayleigh-type and resonant scatterers. Non-ionic species can enhance the heat transfer provided that they reduce the anisotropic and anharmonic vibrational modes of the oxygen atoms. Similarly, the effect of changes in the external conditions applied to the framework materials on the thermal conductivity is determined to some extent by changes in the anharmonicity of the oxygen-atom vibrations.

Another major conclusion of this study is that MD techniques can be employed in the modelling of thermal transport properties of novel and already discovered materials under ambient and extreme conditions, and, therefore, the design of materials with a required set of thermal properties can be foreseen. Further studies of the heat transfer in FAU-topology zeolites, which were not found to undergo phase transformations in the range 100 K $< T <$ 300 K, are in progress.

Acknowledgments

References

[1] Murashov V V 1998 *PhD Thesis* Dalhousie University, Halifax, NS
[2] Murashov V V and White M A 1998 *J. Mater. Sci.* submitted
[3] Horai K 1971 *J. Geophys. Res.* **76** 1278
[4] Meier W H, Olson D H and Baerlocher C 1996 *Atlas of Zeolite Structures* 4th edn (London: Elsevier)
[5] Maeda A and Munakata T 1995 *Phys. Rev.* E **52** 234
[6] Ladd A J C, Moran B and Hoover W G 1986 *Phys. Rev.* B **34** 5058
[7] Inoue R, Tanaka H and Nakanishi K 1996 *J. Chem. Phys.* **104** 9569
[8] Kramer G J, Farragher N P, van Beest B W H and van Santen R A 1991 *Phys. Rev.* B **43** 5068
[9] Murashov V V 1995 *Chem. Phys. Lett.* **236** 609
[10] Parrinello M and Rahman A 1981 *J. Appl. Phys.* **52** 7182
[11] Hoover W 1985 *Phys. Rev.* A **31** 1695
[12] Wyckoff R W G 1963 *Crystal Structures* 2nd edn (New York: Wiley)
[13] Pluth J J and Smith J V 1980 *J. Am. Chem. Soc.* **102** 4704
[14] Bursill L A, Lodge E A, Thomas J M and Cheetham A K 1981 *J. Phys. Chem.* **85** 2409
[15] Hriljac J A, Eddy M M, Cheetham A K and Donohue J A 1993 *J. Solid State Chem.* **106** 66
[16] Hoover W G 1983 *Rev. Phys. Chem.* **34** 103

[17] Evans D J and Morris G P 1984 *Comput. Phys. Rep.* **1** 297
[18] Gillan M J and Dixon M 1983 *J. Phys. C: Solid State Phys.* **16** 869
[19] Vogelsang R and Hoheisel C 1987 *Phys. Rev.* A **35** 3487
[20] Sindzingre P and Gillan M J 1990 *J. Phys.: Condens. Matter* **2** 7033
[21] Touloukian Y A 1970 *Thermophysical Properties of Matter* (New York: Plenum)
[22] Tse J S and Klug D D 1991 *J. Chem. Phys.* **95** 9176
[23] de Boer K, Jansen A P J and van Santen R A 1995 *Phys. Rev.* B **52** 12 579
[24] Petrovic I, Heaney P J and Navrotsky A 1996 *Phys. Chem. Minerals* **23** 119
[25] Hu Y, Navrotsky A, Chen C-Y and Davis M E 1995 *Chem. Mater.* **7** 1816
[26] Spindler K, Griesinger A and Hahne E 1997 *High Temp.–High Pressures* **29** 45
[27] Klemens P G 1958 *Solid State Physics* vol 7 (New York: Academic) p 1
[28] Cahill D G and Pohl R O 1988 *Annu. Rev. Phys. Chem.* **39** 93
[29] Parise J B, Corbin D R and Abrams L 1984 *Acta Crystallogr.* C **40** 1493
[30] Petrovic I, Navrotsky A, Davis M E and Zones S I 1993 *Chem. Mater.* **5** 1805
[31] Couves J W, Jones R H, Parkera S C, Tschaufeserand P and Catlow C R A 1993 *J. Phys.: Condens. Matter* **5** L329
[32] Svishchev I M, Kusalik P G and Murashov V V 1997 *Phys. Rev.* B **55** 721
[33] Hazen R M 1983 *Science* **219** 1065
[34] Ross R G, Andersson P and Backstrom G 1978 *J. Chem. Phys.* **68** 3967
[35] Soga N, Klemas G H and Horai K 1972 *J. Geophys. Res.* **77** 2610
[36] Loewenstein W 1954 *Science* **39** 92
[37] Sierra L, Deroche C, Gies H and Guth J L 1994 *Microporous Mater.* **3** 2923
[38] Philippot E, Goiffon A, Ibanez A and Pintard M 1994 *J. Solid State Chem.* **110** 356
[39] Slack G A 1979 *Solid State Physics* vol 34 (New York: Academic) p 1
[40] Nolas G S, Slack G A and Ehrlich A C 1996 *J. Appl. Phys.* **79** 4002
[41] Morelli D T and Meisner G P 1995 *J. Appl. Phys.* **77** 3777
[42] Nolas G S, Slack G A and Ehrlich A C 1996 *J. Appl. Phys.* **79** 4002
[43] Wybourne M N, Kiff B J and Batchelder D N 1984 *Phys. Rev. Lett.* **53** 580
[44] Tse J S and White M A 1988 *J. Phys. Chem.* **92** 5006
[45] Joffe A F 1956 *Can. J. Phys.* **34** 1342
[46] Smith J V 1974 *Feldspar Minerals* vol 1 (New York: Springer)
[47] Depmeier W 1985 *Acta Crystallogr.* B **41** 101
[48] Berman R 1976 *Thermal Conduction in Solids* (Oxford: Oxford University Press)
[49] Meisner G P, Morelli D T, Hu S, Yang J and Uher C 1998 *Phys. Rev. Lett.* **80** 3551
[50] Simmons G 1969 *Earth Planet. Sci. Lett.* **6** 359
[51] Tse J S, Shpakov V P, Murashov V V and Belosludov V R 1997 *J. Chem. Phys.* **107** 9271
[52] Jameson C J, Jameson A K, Baello B I and Lim H-M 1994 *J. Chem. Phys.* **100** 5965